Stochastic properties of cat auditory nerve responses to electric and acoustic stimuli and application to intensity discrimination

Eric Javel and Neal F. Viemeister
Departments of Otolaryngology and Psychology, University of Minnesota, Minneapolis, Minnesota 55455

(Received 26 October 1998; revised 24 August 1999; accepted 17 September 1999)

Statistical properties of electrically stimulated (ES) and acoustically stimulated (AS) auditory nerve fiber responses were assessed in undeafened and short-term deafened cats, and a detection theory approach was used to determine fibers' abilities to signal intensity changes. ES responses differed from AS responses in several ways. Rate-level functions were an order of magnitude steeper, and discharge rate normally saturated at the stimulus pulse rate. Dynamic ranges were typically 1–4 dB for 200 pps signals, as compared with 15–30 dB for AS signals at CF, and they increased with pulse rate without improving threshold or changing absolute rate-level function slopes. For both ES and AS responses, variability of spike counts elicited by repeated trials increased with level in accord with Poisson-process predictions until the discharge rate exceeded 20–40 spikes/s. AS variability continued increasing monotonically at higher discharge rates, but more slowly. In contrast, maximum ES variability was usually attained at 100 spikes/s, and at higher discharge rates variability reached a plateau that was either maintained or decreased slightly until discharge rate approached the stimulus pulse rate. Variability then decreased to zero as each pulse elicited a spike. Increasing pulse rate did not substantially affect variability for rates up to 800 pps; rather, higher pulse rates simply extended the plateau region. Spike count variability was unusually high for some ES fibers. This was traced to response nonstationarities that stemmed from two sources, namely level-dependent fluctuations in excitability that occurred at 1–3 s intervals and, for responses to high-rate, high-intensity signals, fatigue that arose when fibers discharged at their maximum possible rates. Intensity discrimination performance was assessed using spike count as the decision variable in a simulated 2IFC task. Neurometric functions (percent correct versus intensity difference) were obtained at several levels of the standard (I), and the intensity difference (ΔI) necessary for 70% correct responses was estimated. AS Weber fractions ($10 \log \Delta I/I$) averaged $+0.2$ dB ($\Delta I_{\mathrm{dB}} = 3.1$ dB) for 50 ms tones at CF. ES Weber fractions averaged -12.8 dB ($\Delta I_{\mathrm{dB}} = 0.23$ dB) for 50 ms, 200 pps signals, and performance was approximately constant between 100 and 1000 pps. Intensity discrimination by single cells in ES conditions paralleled human psychophysical performance for similar signals. High ES sensitivity to intensity changes arose primarily from steeper rate-level functions and secondarily from reduced spike count variability. [S0001-4966(99)07912-6]

PACS numbers: 43.64.Me, 43.64.Pg, 43.66.Ba [RDF]

INTRODUCTION

A major problem in hearing mediated by cochlear implants is the limited dynamic range over which useful information can be presented. The typical dynamic range in implanted humans is 4–10 dB for brief (100–200 μs phase) biphasic pulses presented to bipolar electrodes (Donaldson *et al.*, 1997), and it seldom exceeds 20 dB (Shannon, 1993). This is in sharp contrast with the dynamic range of more than 100 dB for normal acoustic hearing. Various compression schemes are used in implant processors in an attempt to map the useful acoustic range to the limited electric range. A potential problem with compression is that it may render important amplitude changes inaudible. The seriousness of this problem would be mitigated if sensitivity to intensity changes were significantly greater in electric hearing than in acoustic hearing. Psychophysical data indicate that intensity difference limens (DLs) in implanted humans vary considerably among subjects but are not appreciably smaller than those observed in normal acoustic hearing (Nelson *et al.*, 1996).

Intensity coding mechanisms for electric stimulation (ES) can be inferred from auditory nerve fiber (ANF) responses, but the data are too limited to permit much insight. It is known that ES rate-level functions are much steeper than those for acoustic stimulation (AS), dynamic range is correspondingly smaller, and dynamic range depends on stimulus pulse rate (Moxon, 1971; Hartmann *et al.*, 1984; Javel, 1990; Dynes and Delgutte, 1992). Steeper rate-level functions alone suggest that intensity discrimination should be much better for ES than for AS, since a smaller intensity increment would be needed to achieve a criterion change in discharge rate. However, it is generally thought that the psychophysical ability to discriminate intensity also depends on variability in responses to nominally identical stimuli. Such variability or ''internal noise'' is a characteristic of sensory

processing and is incorporated in all recent models of acoustic intensity discrimination.

Response variability in ES has only begun to be considered (Bruce *et al.*, 1999), and the role it plays in perceptual processing is not well understood. The impact of stochastic response properties in intensity discrimination by ANFs can be investigated directly using a simulated psychophysical task (Relkin and Pelli, 1987). Although such analyses have provided insights into basic aspects of intensity coding in AS conditions (Delgutte, 1987; Viemeister, 1983, 1988; Winslow and Sachs, 1988; Winter and Palmer, 1991), no comparable analyses exist for ES.

Several investigators have incorporated random noise sources into single-cell models for ES as a way of introducing probabilistic response behavior (Verveen, 1962; White *et al.*, 1987; Bruce *et al.*, 1999). Although this approach produces the needed effects, the stochastic properties of the noise and the effects of absolute and relative refractoriness, both of which affect the form of the variance function, are still uncertain. Bruce *et al.* (1997) took stochastic behavior into account in developing a neural population model for ES, and they applied it to intensity discrimination. However, their model was based on limited physiological data from undeafened and acutely deafened ears. It is not clear that the same results would have been obtained if model neurons were based on responses from chronically deafened cochleas, in which fibers often exhibit degraded stimulus coding capabilities (Shepherd and Javel, 1997).

Chronic deafness leads to variable, time-dependent loss of spiral ganglion cell peripheral processes, cell death, and reduction of average central-process axon caliber in surviving cells (Leake and Hradek, 1988; Spoendlin and Schrott, 1989). Biophysical models of neuronal excitability to electric stimuli predict an inverse relationship between response variability and the diameter of the node of Ranvier at the active spike initiation site, and they predict a direct relationship between node diameter and rate-level function slope (Verveen, 1962). Loss of peripheral processes necessarily causes spike initiation sites to shift to central processes, and, on average, central processes have larger diameters than peripheral processes (Liberman, 1980; Liberman and Oliver, 1984). This implies steeper, rate-level functions and reduced response variability, which translates into smaller intensity difference limens. On the other hand, deafness-induced reductions in average central-process caliber implies shallower rate-level functions and higher variability, and cell loss implies that fewer spikes are available for perceptual decision-making. These effects would increase intensity difference limens. Thus chronic deafness can have opposite effects on ES intensity discrimination.

The first part of this paper examines variability in ANF responses, with a particular emphasis on the statistical properties of driven activity. It will be shown that spike count variability behaves differently in ES than in AS, with ES variability typically being much smaller. It will also be shown that increasing pulse rate generally does not increase variability, at least for pulse rates up to 800 pps, and that some ES fibers exhibit time-dependent fluctuations in excitability, the effect of which is to increase variability.

The second part examines the role spike count variability plays in intensity coding. A detection theory approach is used to examine ANF's abilities to signal intensity changes, and single-cell performance is related to psychophysical performance in humans. It will be shown that fibers' abilities to discriminate intensity are substantially better in ES than in AS, and that steeper slopes of rate-level functions and decreased variability of spike counts both contribute to the effect. It will also be shown that single-cell performance matches perceptual findings in implanted humans relatively well, but it falls somewhat short of accounting for performance in normal acoustic hearing.

I. METHODS

Single ANF responses to electric and acoustic stimuli were recorded in cats. All AS animals and six ES animals possessed normal hearing prior to the experiment. Three other ES animals were deafened 6–12 weeks prior to single-unit experiments by co-administering kanamycin and ethacrynic acid in a single session (Xu *et al.*, 1993). This method effectively eliminates outer and inner hair cells, as evidenced by a lack of acoustic responsiveness and no random spontaneous activity in the great majority of fiber responses. It also produced 20%–40% peripheral process loss in the basal cochlear turn by 12 weeks post-deafening. One other ES animal was profoundly deafened as a kitten by serial kanamycin administration and experimented upon 3.7 years later.

Animals were anesthetized with pentobarbital (40 mg/kg, IM) and tracheostomized, and the animal's head was mounted in a stereotaxic frame. The skull overlying the lateral posterior fossa was exposed and opened, and a portion of the cerebellum was aspirated to reveal the cochlear nucleus and brainstem. Small cotton pledgets were wedged between the brainstem and skull wall to expose the eighth nerve at its point of exit from the internal auditory meatus. A Davies chamber was affixed to the skull, filled with warmed mineral oil, and sealed by a clear plastic cover plate on which a miniature hydraulic microdrive (FHC, Inc.) was mounted. The microdrive carried a 3M KCl-filled recording micropipette with an ac impedance of 20–30 MΩ at 1 kHz. The tip of the micropipette was visually positioned over the eighth nerve using an operating microscope, and the electrode was advanced into the nerve with a remote-controlled stepping motor.

ES animals were acutely implanted with a custom-built electrode array that was a smaller-diameter version of a Nucleus (Cochlear Corp.) implant. It possessed 0.3 mm platinum bands on 0.75 mm centers. Band diameters decreased from 0.6 mm at the basal end to 0.4 mm at the tip. To install the array, the bulla was opened from a posterolateral direction, the round window membrane was excised, and the array was gently inserted into scala tympani to a depth of approximately 6 mm. This located the apical-most band nominally at the 15 kHz cochlear place (Liberman, 1982).

Custom software was used to specify stimulus sequences consisting of digitally synthesized 50–100 μs phase biphasic pulse trains (ES animals) or CF tones (AS animals). The digital-to-analog conversion rate was 100–200 kHz. For AS

signals, conversion rates were chosen to put all aliased spectral components above 60 kHz. Unit activity was detected with probe stimuli consisting of 100 pps pulse trains presented at 1–2 mA in ES animals and 100 ms wide-band noise bursts presented at 70–80 dB SPL in AS animals. ES responses were obtained to pulse trains presented at user-specified rates, typically 200 pps, through an isolated voltage-to-current converter (Bak). ES signals were delivered in 50–400 ms trains to a bipolar electrode pair consisting of the most apical band and the second-or third-most apical band. AS signals were sinusoids of 50 ms duration presented through a calibrated Beyer DT-48 earphone in a closed system. The duty cycle was 25%–50% for ES signals and 33% for AS signals. Single-fiber responses were collected as input–output functions for 20–200 repetitions of signals presented in increasing order of intensity. Step sizes were 0.2–0.5 dB for ES signals and 5 dB for AS signals.

Action potentials recorded by the micropipette were amplified (WPI Instruments) and displayed on an oscilloscope. Stimulus artifact caused by ES signals was eliminated by microprocessor-controlled sample-and-hold blanking that began at pulse onset and was maintained for a user-specified time, normally slightly longer than the duration of the pulse. The rising phases of spikes were voltage discriminated using the oscilloscope's trigger circuit. Trigger pulses coincident with the onset of each oscilloscope sweep were led to custom timing hardware. Custom software was used to time incoming spikes to 10 μs accuracy and to analyze and display neural responses in real time.

Detailed information about methods, numbers of fibers recorded from each ES animal, and post-deafening cochlear morphology is provided in Shepherd and Javel (1997). ES responses described here are representative of data obtained from 200 fibers in undeafened ears and 158 fibers in deafened ears. AS responses shown here are based on data obtained from 43 fibers in one animal and are representative of similar data from several other animals. Protocols were reviewed and approved by the Creighton University Animal Care and Use Committee.

II. RESULTS

A. ANF responses

Representative raw and normalized rate-level functions for ES and AS conditions are shown in Fig. 1. ES and AS responses came from different animals, but data in each set came from the same ear. The ES data were obtained from a cat profoundly deafened for eight weeks prior to the single-cell experiment. They have been selected to show the range of thresholds and dynamic range that are typically encountered. Responses were elicited by 100 μs phase, 200 pps biphasic pulse trains presented for 50 ms. The curves in the lower left panel of Fig. 1 show the same data as in the upper left panel, except that threshold has been normalized to 0 dB and discharge rate is expressed as a percentage of the maximum expected rate of 200 spikes/s. We define threshold as the intensity eliciting a discharge rate of 10% of the maximum driven rate. For 200 pps signals this is 20 spikes/s.

AS responses are shown on the right side of Fig. 1 for comparison with the ES responses. These were selected on the basis of similar characteristic frequency (CF), except for the fibers with extremely high and low spontaneous rates, which were included for completeness. The responses exhibit typical variation in threshold and spontaneous and maximum discharge rates. Normalized responses (lower right panel) show that slopes are comparable across spontaneous rate (Sachs and Abbas, 1974), and some fibers exhibit sloping saturations (Sachs *et al.*, 1989).

Consistent with earlier reports (Moxon, 1971; Hartmann *et al.*, 1984; Javel *et al.*, 1987; Dynes and Delgutte, 1992), most ES fibers exhibited dynamic ranges of 1–4 dB. We define dynamic range as the intensity range over which discharge rate increases from 10% above the spontaneous rate to 90% of the maximum rate. While 1–4 dB dynamic ranges are typical for ES, they are much smaller than the 15–30 dB dynamic ranges normally observed in AS at CF.

Pulse-number distributions (PNDs) are one of several measures of stochastic behavior (Teich and Khanna, 1985). These are formed by plotting the proportion of times a fixed signal elicits a particular spike count. Representative PNDs for ES and AS conditions are shown by solid lines in Fig. 2. The dashed lines are the PNDs predicted by a Poisson process with the same mean rate as the corresponding neural data. The probability density function for a Poisson process is defined by $P=(\mu^N e^{-\mu})/N!$, where P is proportion of occurrences, μ is the mean count (discharge rate times duration), and N is the number of counts. Although it is known that variability of AS responses deviates from Poisson-process predictions because of absolute and relative refractoriness (Gray, 1967; Gaumond *et al.*, 1982; Johnson and Swami, 1983; Young and Barta, 1986), Poisson-process expectations form a convenient reference to which ES and AS response behavior may be compared. Figure 2 shows that distributions of AS and ES spike counts both deviate progressively more from Poisson-process predictions as discharge rate increases, and that ES variability is smaller than AS variability over most of the dynamic range.

Further information on spike count variability is provided in Fig. 3. These data came from the fibers whose rate-level functions were shown in Fig. 1, and the same symbols have been carried forward. The AS data (right panel) indicate that Poisson-process predictions (variance=mean and s.d. $=\sqrt{\text{mean}}$, denoted by the solid line) are maintained up to 1–2 counts per 50 ms trial or discharge rates of 20–40 spikes/s, and that variability falls increasingly short of Poisson-process predictions at higher discharge rates. Responses of fibers with different spontaneous rates all follow the same general trend. This implies that variability depends primarily on overall rate. Important aspects of the AS responses are that variability increases monotonically with level and that discharge rate saturation has no obvious effect on variability.

The ES data shown in the left panel of Fig. 3 also follow Poisson-process predictions up to 20–40 spikes/s and then depart at higher discharge rates. However, notable differences exist between ES and AS data. First, once ES variability departs from Poisson-process expectations, it tends to remain at a constant value or ''plateau'' until discharge rate

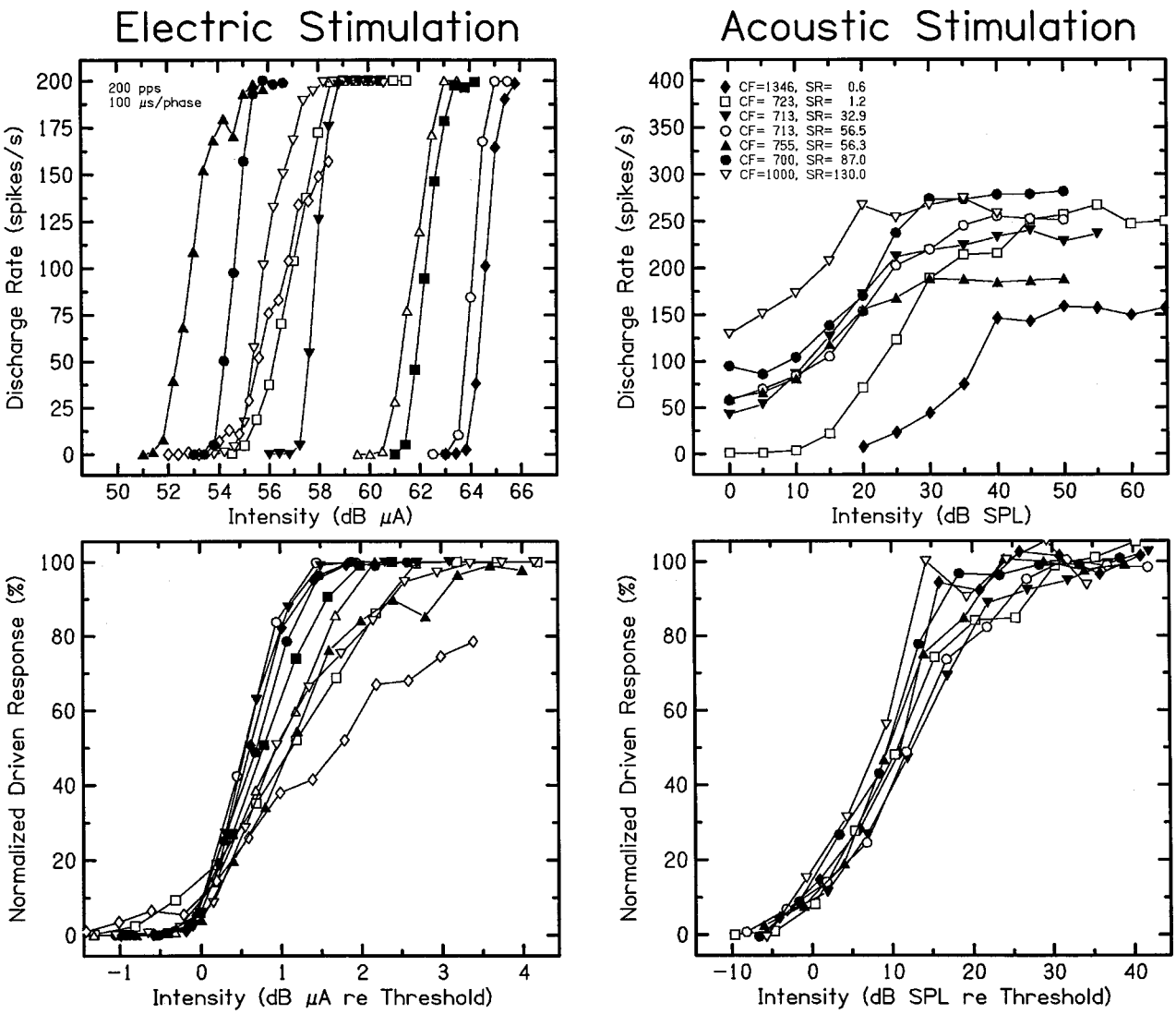

FIG. 1. Representative rate-level functions for ES at 200 pps (left) and AS at CF (right). Each set of functions came from the same ear. Raw rate-level functions are shown in the top row. The same functions, normalized for both discharge rate and intensity relative to threshold, are shown in the bottom row. SR denotes spontaneous rate.

approaches the stimulus pulse rate, in this case 200 pps or 10 counts per 50 ms trial. And second, variability rapidly decreases to zero when discharge rate approaches the stimulus pulse rate and responses become deterministic, i.e., every pulse elicits a spike.

The AS data in Fig. 3 resemble those reported by Young and Barta (1986), but average variability is slightly lower. The discrepancy stems from differences in the counting intervals. That is, Young and Barta considered only the steady-state portion of the response, and they purposely excluded spikes occurring during the (nonstationary) rapid and short-term adaptation periods at response onset (Westerman and Smith, 1984). Our data, on the other hand, include these spikes because the ''perceptual processor'' likely uses them. Analyses we performed on AS data, not shown here, indicated that the elevated discharge rates at response onset have relatively low variability. Although low variability at signal onset reduces overall variability, the effect is small for signals with all but the shortest durations. As evidence of this, one may note the similarity between Winter and Palmer's (1991) and Young and Barta's (1986) variability data, obtained using different counting intervals.

Figure 4 shows rate-level functions and variability data for signals presented at pulse rates ranging from 100 to 800 pps. Data for three fibers are shown. One fiber came from an undeafened ear, one came from an ear profoundly deafened for eight weeks prior to experimentation, and one came from an ear profoundly deafened for 3.7 years. Rate-level functions exhibit differences in slope across fibers. The fiber from the undeafened ear (top row) exhibits the type of response seen most often, i.e., a discharge rate that saturates at the pulse rate, no improvement in threshold with increasing pulse rate, and rate-level function slopes that remain constant in absolute terms (spikes/s/dB). The dependence of saturation rate on pulse rate produces a corresponding increase in dynamic range.

Discharge rates in the fiber from the eight-week-deafened ear (middle row) also saturated at the stimulus pulse rate, but thresholds increased with pulse rate. However, at least some of the threshold increase may be artifactual due

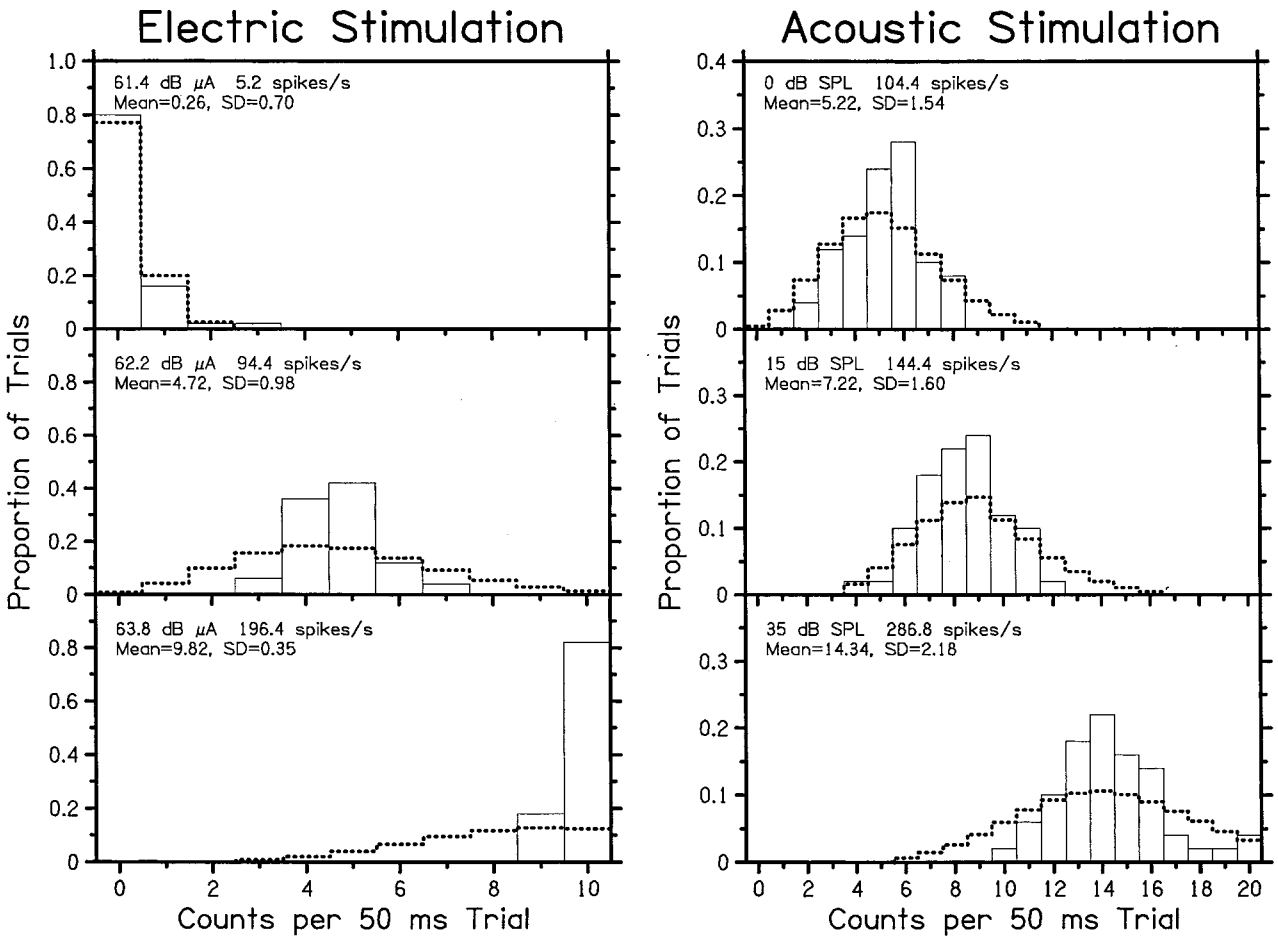

FIG. 2. PNDs obtained from ANFs at three intensities for ES at 200 pps (left) and AS at CF (right). Dashed lines denote the distribution of counts predicted by a Poisson process at the obtained mean rates.

to the fact that responses were collected in increasing order of intensity and pulse rate. That is, data at low intensities and high pulse rates were collected just after the fiber had finished responding at high discharge rates to the next-lower pulse rate, and the fiber may have been temporarily fatigued. Other fibers from this ear exhibited similar threshold increases with increasing pulse rate. Unlike either of the other two, the fiber from the long-term-deafened ear (bottom row) displayed large dynamic ranges and was unable to discharge at rates higher than 500–600 spikes/s.

The behavior of spike count variability for these fibers is shown in the right-hand column of Fig. 4. Variability initially increased with discharge rate in accord with Poisson-process predictions, and it deviated from predicted behavior when rates exceeded 20–40 spikes/s. This is similar to behavior shown previously in Fig. 3 for 200 pps signals. Variability decreased somewhat when the discharge rate exceeded 100 spikes/s, and it maintained a plateau value until the discharge rate approached the stimulus pulse rate. Variability increased at high pulse and discharge rates for the fibers from the undeafened and long-term-deafened ear, but not for the fiber from the short-term-deafened ear.

The point at which variability increases at high pulse rates and intensities appears to be related to the maximum sustained discharge rate a given fiber can generate. In Fig. 4, increases in spike count variability occurred at 700 spikes/s for the fiber from the undeafened ear and at 450 spikes/s for the fiber from the long-term-deafened ear. These were the highest sustained rates elicitable from those fibers. Absence of a variability increase for the fiber from the short-term-deafened ear likely stemmed from that fiber's ability to discharge at very high rates. Although it was not examined, we suspect that this particular fiber was capable of discharging in a sustained manner at rates >800 spikes/s.

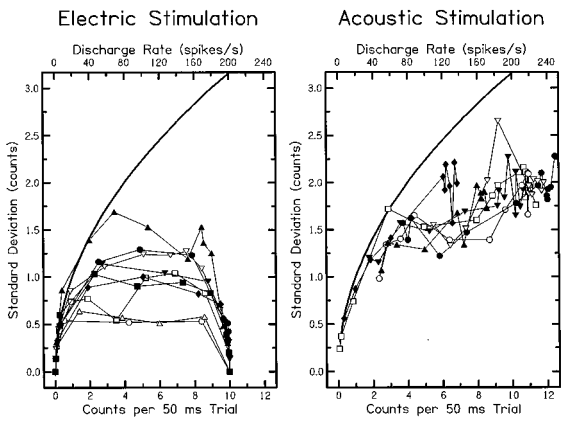

FIG. 3. Representative variability functions for ES at 200 pps (left) and AS at CF (right). Functions are from the same fibers whose rate-level functions are shown in Fig. 1, using the same symbols.

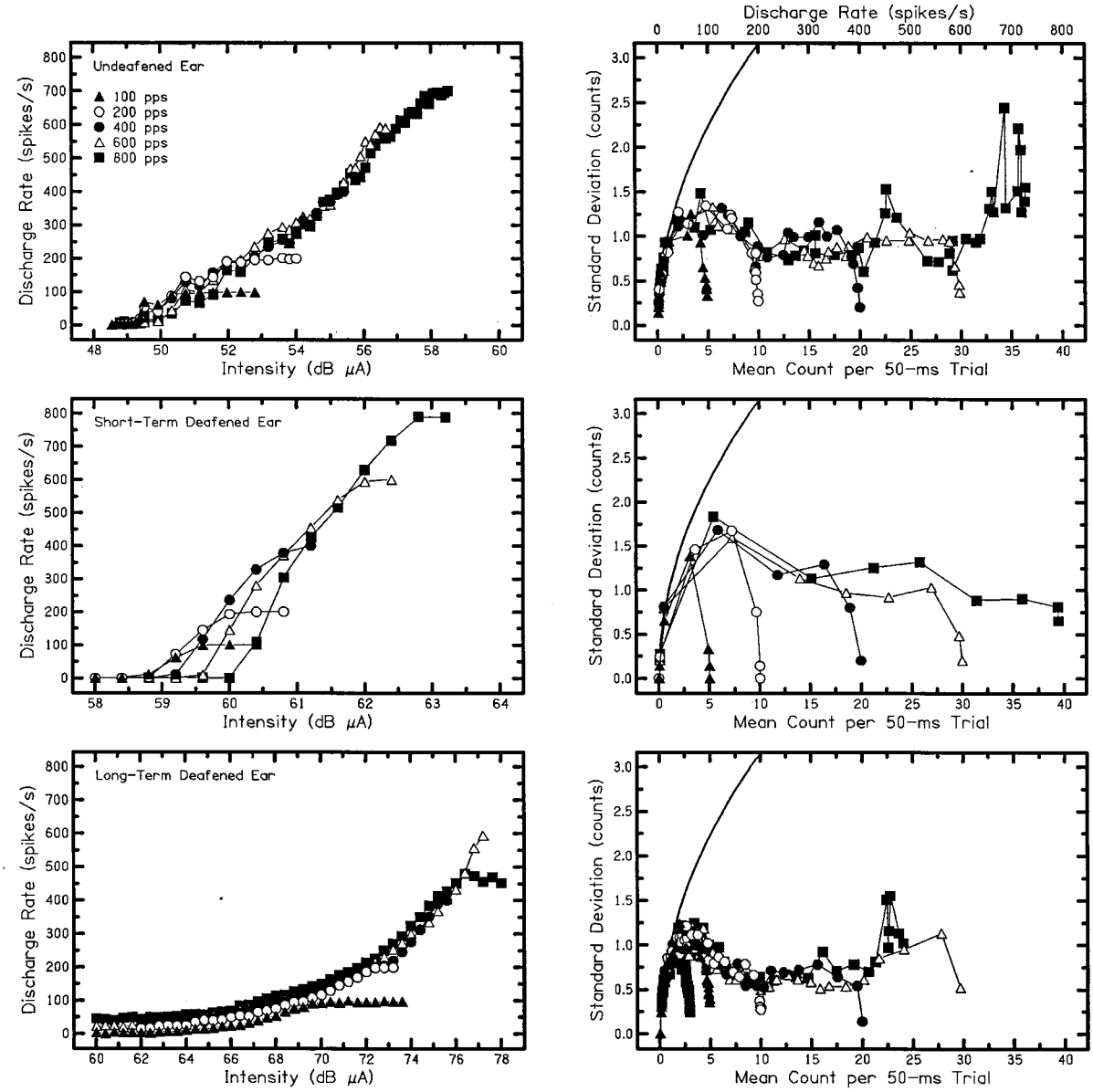

FIG. 4. Rate-level functions (left) and variability-count functions (right) for three ES fibers stimulated at pulse rates ranging from 100 to 800 pps.

Maximum discharge rates and variability of responses from other fibers in all three types of ear were distributed over a range similar to that shown in Fig. 4. That is, some fibers could discharge at high sustained rates, and consequently variability did not increase when stimuli at 800 pps elicited discharge rates of 800 spikes/s. However, other fibers could not discharge at high rates, and variability increased when discharge rate approached the maximum possible. Differences among fibers likely stem from variation in the duration of the absolute refractory period and the time constant for recovery from relative refractoriness. These differences exist in undeafened as well as short-term-deafened and long-term-deafened ears.

Distributions of maximum spike count variability observed for 50 ms, 200 pps signals are shown in the left-hand column of Fig. 5. They were obtained by forming a variability function for each fiber and noting the highest standard deviation. As previously indicated in Figs. 3–4, maximum ES variability normally occurs at 2–5 counts per 50 ms trial, or 40–100 spikes/s. Spike count variability in our sample formed two subtypes. One type, indicated in the upper left panel, displayed low variability. The other type, indicated in the lower left panel, exhibited variability that spanned a wide, generally high range. As discussed later, the two subtypes differed in the extent to which excitability varied from trial to trial. The dashed lines are a reference. They indicate the Poisson-process prediction that a mean count of 3 (corresponding to 60 spikes/s for a 50-ms trial) should possess a standard deviation of 1.73 counts. The data in Fig. 5 indicate that, like AS fibers, most ES fibers from deafened ears show less spike count variability than a Poisson process predicts, but a subset of fibers exhibits greater variability. Although our sample size is too small to draw firm conclusions, increased variability appears to be more prevalent in short-term-deafened animals, and a larger proportion of fibers exhibit high variability as duration of deafness increases. In our

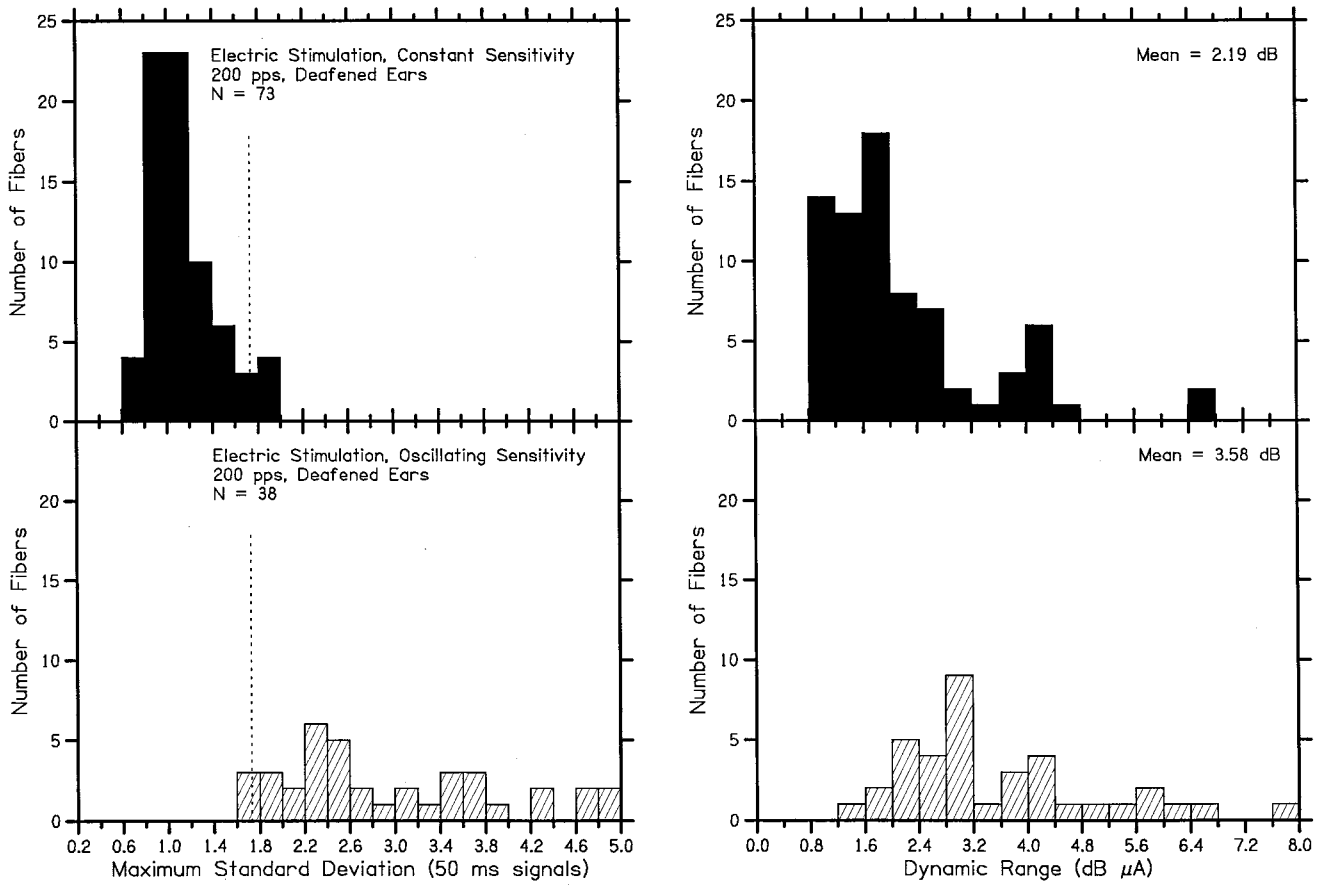

FIG. 5. Left: Distributions of maximum spike count variability for 50 ms, 200 pps stimuli from ES fibers in deafened ears whose excitability remained constant during data collection (top) and fibers whose excitability fluctuated over time (bottom). Right: Dynamic ranges of ES fibers with constant (top) and fluctuating (bottom) excitability.

sample, 34.3% of all fibers from short-term-deafened ears exhibited increased variability, but the proportion increased from 28% to 42% between 6 and 12 weeks post-deafening. In contrast, fibers exhibiting increased spike count variability were rarely encountered in either undeafened or long-term-deafened ears. Thus increased variability appears to be associated with active cochlear degeneration.

The right-hand panel of Fig. 5 shows distributions of dynamic range for the same fibers whose variability is depicted in the left-hand panel. These data indicate that ES fibers with high spike count variability also possess larger dynamic ranges than fibers with low variability (3.58 dB vs 2.19 dB). Differences between subtypes were statistically significant for both variability ($t=10.11$, $df=40.8$, $p<0.001$) and dynamic range ($t=4.86$, $df=60.0$, $p<0.001$).

Examples of rate-level and variability functions for ''high variability'' fibers are shown in Fig. 6. These data all came from the same eight-week-deafened ear. The rate-level functions had typical shapes but larger than normal dynamic ranges. However, in each case maximum spike count variability exceeded Poisson-process expectations for mean counts <7 per 50 ms, or <140 spikes/s. Further examination of these responses and others like them showed that in every case increased spike count variability was associated with periodic fluctuations in sensitivity. We call this phenomenon ''oscillating excitability.'' An analysis of responses to 200 pps pulse trains in a fiber from an eight-week-deafened cat is shown in Fig. 7. The fiber's rate-level function (upper left) displayed a rather broad dynamic range of 5.25 dB, and spike count variability (lower left) greatly exceeded Poisson-process predictions. Dot rasters (middle column) indicated that at near-threshold intensities the fiber only responded at 3 s intervals. As intensity increased the period of the response oscillations decreased to about 1 s, then progressively filled in, culminating in the fiber ultimately producing a spike for

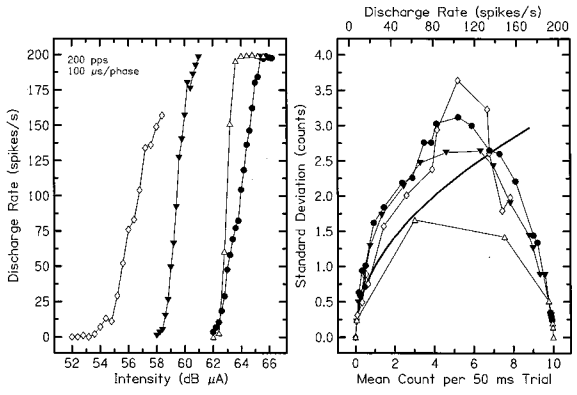

FIG. 6. Rate-level (left) and variability-count functions (right) for four fibers that exhibited oscillating excitability. All the fibers came from the same chronically deafened ear.

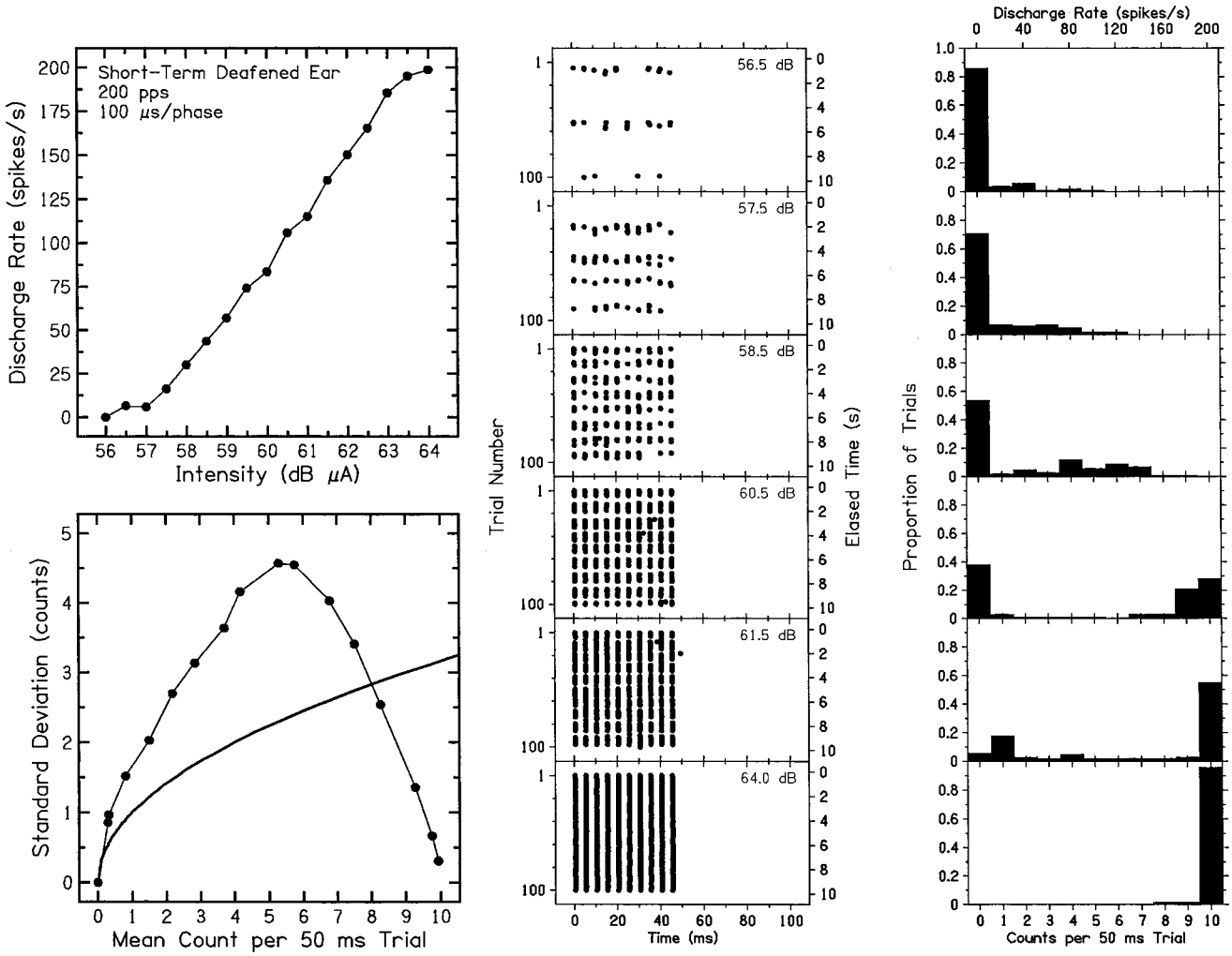

FIG. 7. Rate-level function (top left), variability-count function (bottom left), selected dot rasters (center), and PNDs (right) for a fiber that exhibited oscillating excitability. The fiber came from a chronically deafened ear.

every stimulus pulse. PNDs (right column) show two modes at intensities in which excitability fluctuated, corresponding to alternating periods of activity and inactivity. The large range of counts elicited by repeated trials explains the high spike count variability. Although the observation that fluctuations in excitability disappeared at high intensities is seemingly enough to rule out the possibility that the phenomenon is artifactual, we nonetheless performed several tests to prove that oscillating excitability did not arise from movement due to heart or respiration rate. It appears to be an intrinsic property of ANF responses that is especially prevalent in recently de-afferented ears, and fibers exhibiting the phenomenon were interspersed along the same electrode track with fibers whose trial-to-trial excitability remained constant. Thus ''oscillating excitability'' is one form of nonstationarity that causes increased variability in ES fiber responses. Its origin is unclear.

We also observed a second form of nonstationarity in ES fiber responses that occurred only at very high discharge rates. This consisted of a fatiguelike phenomenon in which discharge rate progressively decreased during a data collection run, leading to greater spread in PNDs and higher variability. Results of one analysis are provided in Fig. 8, which shows summaries of responses from an ES fiber in an undeafened ear that was stimulated by 800 pps trains at 58.3 dB μA for 50 trials of 100 ms duration. The left-hand panel shows running averages for mean count (solid line referred to left-hand axis) and spike count variability calculated over the 50-trial run (dashed line referred to right-hand axis). The discharge rate was initially high (760–770 spikes/s) and decayed with time to an overall rate of 680 spikes/s. Variability moved in the opposite direction, being initially low and increasing with time. Although the overall standard deviation of approximately 4 counts per 100 ms was considerably lower than Poisson-process predictions at 67–70 counts, namely 8.2–8.4 counts, it is nonetheless high for ES activity.

Analyzing these responses in five-trial blocks produced the data shown in the right-hand panel of Fig. 8. The discharge rate decreased by 100 spikes/s over the first 20–25 trials and then remained relatively constant. However, standard deviation in each five-trial block was only 1–2 counts per 100 ms. This is within the range of standard deviations observed at lower pulse rates (cf. Fig. 5). Thus increased spike count variability over the entire duration of the run stemmed from a progressive decrease in discharge rate over time, but moment-to-moment variability was considerably smaller.

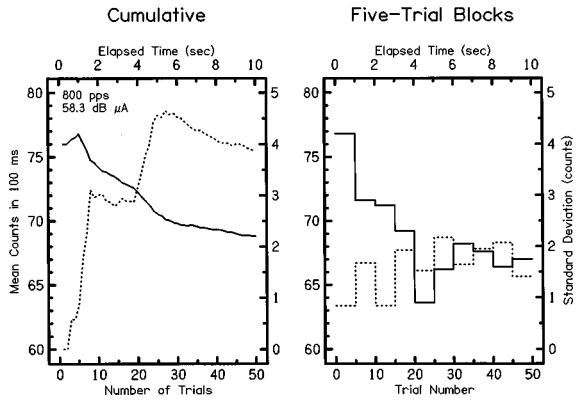

FIG. 8. Behavior of spike counts and their variance as a function of time. Left: Cumulative mean counts (solid line referred to left axis) and spike count variance (dashed line referred to right axis) over 50 presentations of a 100 ms ES signal at 800 pps signal and 58.3 dB μA. Right: The same data, plotted in five trial blocks. Discharge rate decreased from 770 spikes/s to 670 spikes/s during the course of the run. Variance did not change much from moment to moment, but fatigue increased overall variance substantially.

B. Intensity discrimination

The ability of ES and AS fibers to signal intensity differences was assessed in a simulated two-interval-forced-choice (2IFC) intensity discrimination task. Proportion correct discrimination $[P(C)]$ was estimated by computing the proportion of times the number of spikes elicited by a higher-intensity presentation $(I+\Delta I)$ exceeded the number elicited by the standard (I), for each pairing of stimulus presentations in the 20–200 set of trials. When the counts were equal, the number of correct responses was increased by 0.5, corresponding to a ''guess.'' Estimating performance this way avoids assumptions about the form of the probability distributions of counts and thus is advantageous over other measures, such as those based on d'. Although we did not make a detailed comparison, it appears that $P(C)$ based on d' (using means and standard deviations such as those shown in Figs. 3–4) is nearly identical to the direct estimation of $P(C)$ used here.

For a given value of I, a ''neurometric function'' (Movshon *et al.*, 1982; Relkin and Pelli, 1987) was constructed by estimating $P(C)$ for increasing values of ΔI. A sample of neurometric functions for ES and AS is shown in the upper and lower panels, respectively, of Fig. 9. ES stimuli were 200 pps pulse trains, and data are from fibers in two short-term-deafened ears. The fiber whose responses are indicated by unfilled inverted triangles exhibited oscillating excitability, and it was stimulated by 100 ms signals repeated at 200 ms intervals. The other fibers exhibited constant excitability and were stimulated by 50 ms signals repeated at 100 ms intervals. AS stimuli were 50 ms CF tones, repeated at intervals of 150 ms. The parameter is pedestal intensity I. In principle, these functions can be directly compared with psychometric functions for intensity discrimination by human observers. Unfortunately, neither the present data nor the human data are sufficiently detailed to make such a comparison informative.

The level difference at threshold $[\Delta I_{\mathrm{dB}}=10\log(1+\Delta I/I)]$ necessary for $P(C)=0.7$ was estimated from the

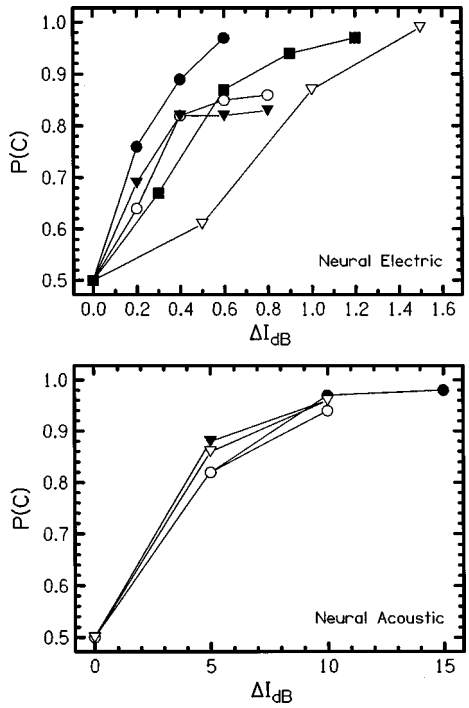

FIG. 9. Neurometric functions obtained in a simulated 2IFC intensity discrimination task in ES (top) and AS (bottom) conditions. ES stimuli were 50 ms presentations of 200 pps pulse trains, and AS stimuli were CF tones (AS). $P(C)$ is the proportion of times the number of counts elicited by a higher-intensity presentation $(I+\Delta I)$ exceeded the number elicited by the standard (I). If counts were equal, the response was taken to be correct with $P(C)=0.5$. Different symbols denote data from different fibers.

neurometric functions at each value of I. Thresholds were computed only when there were at least two points for which $P(C)$ was between 0.6 and 0.9 and were based on linear interpolation between the points closest to $P(C)=0.7$.

The upper panel of Fig. 10 shows Weber functions for several ES fibers from deafened ears. Discrimination thresholds have been converted to Weber fractions $(\Delta I/I)$ and are expressed in dB. This measure is preferable to ΔI_{dB} primarily because it is considerably less compressive. For reference, corresponding values of ΔI_{dB} are shown on the (nonlinear) right axis. At low intensities the Weber fraction for a given fiber increases with decreasing I, i.e., performance becomes worse as intensity decreases. This simply reflects absolute threshold. That is, when I is lower than the absolute threshold, there is no response to the standard and ΔI at threshold corresponds to the difference between the (constant) absolute threshold and signal intensity. At high intensities the discharge rate saturates and the Weber fraction becomes indeterminate because no intensity increase produces a reliable increase or decrease in spike count.[1] The rightmost points for each Weber function approximately reflect the saturation intensity. They essentially define the upper limit of the useful dynamic range for each fiber.

The Weber fraction is approximately constant when I is within the fiber's dynamic range. Some fibers exhibited greater sensitivity to intensity changes, for example, the fiber whose responses are indicated by inverted triangles. Ignoring this fiber, the smallest Weber fractions across fibers are generally seen at larger values of I. This trend suggests that

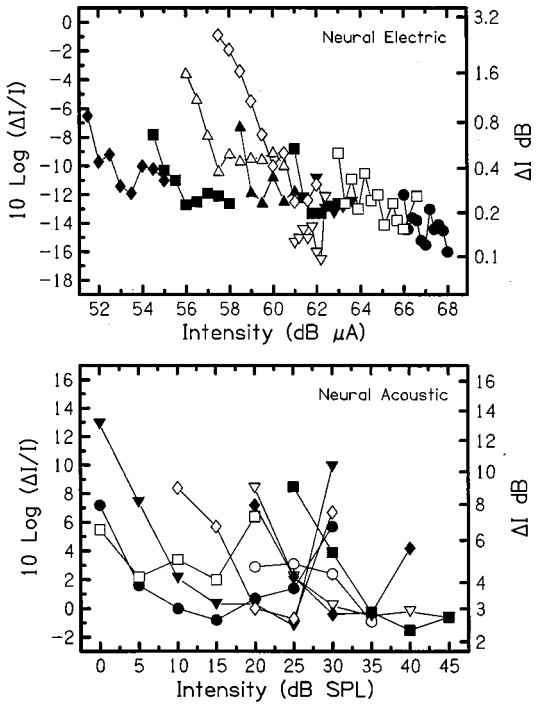

FIG. 10. Weber functions for intensity discrimination of 50 ms signals by several fibers in ES (top) and AS (bottom) conditions. Electric stimuli were 200 pps pulses, and AS stimuli were CF tones. Different symbols denote data from different fibers. Discrimination thresholds [$P(C)=0.7$] have been converted to Weber fractions ($\Delta I/I$) and are expressed in dB. Corresponding values of ΔI_{dB} are shown on the (nonlinear) right vertical axis for reference purposes.

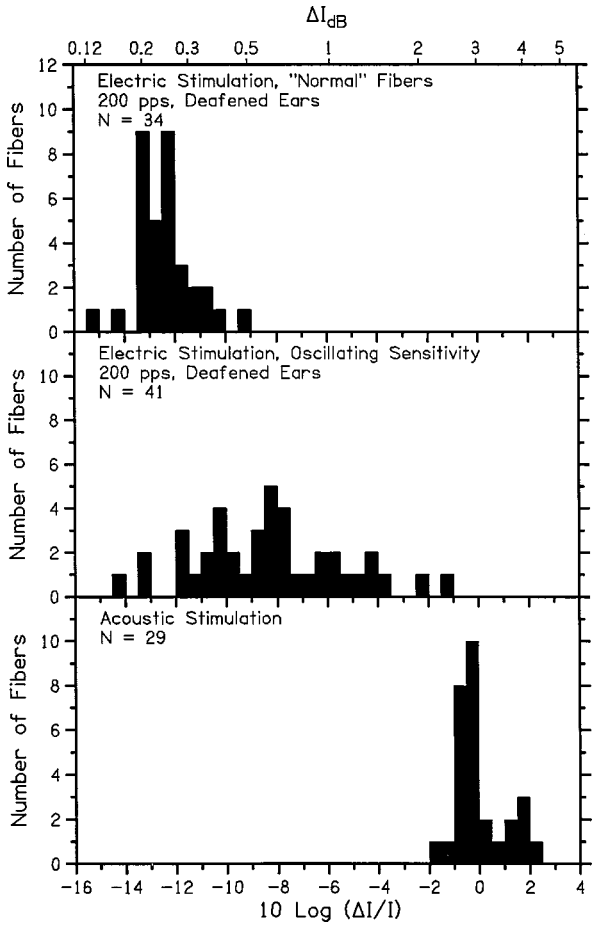

FIG. 11. Distributions of Weber fractions for intensity discrimination by ES fibers that did not exhibit oscillating excitability (top), ES fibers that did (middle), and AS fibers (bottom). ES signals were at 200 pps, and AS signals were at CF. Signal duration was 50 ms, and all AS fibers came from the same ear.

fibers with higher absolute thresholds may be slightly more sensitive to intensity changes. It is consistent with the notion that high-threshold neurons are stimulated on their central processes, which in turn have larger node diameters, steeper rate-level functions, and lower membrane noise. Sensitivity to intensity changes should also correlate with latency, which is generally shorter for central-process activation sites than for peripheral-process activation sites (Javel and Shepherd, 1999).

Weber functions for intensity discrimination in AS conditions are shown in the lower panel of Fig. 10. Stimuli were 50 ms CF tones repeated at 150 ms intervals, and all responses came from the same ear. The data are similar to those previously reported by Delgutte (1987) and Viemeister (1988), and the AS functions are presented here because (1) data were obtained under conditions closely comparable to those for ES and (2) the analysis was identical. Two major differences exist between the AS data and the ES data. As would be expected from the rate-level functions, the range over which performance improves is considerably larger for AS than for ES (note the difference in *X*-axis scales between the two panels in Fig. 10). More importantly, the asymptotic values for Weber fractions in ES are considerably smaller than the minimum values for AS.

Distributions of Weber fractions for ES and AS conditions, averaged over values obtained within each fiber's dynamic range, are shown in Fig. 11. Responses of ES fibers whose excitability remained constant across time are shown at the top; responses of ES fibers exhibiting oscillating excitability are shown in the middle; and responses of AS fibers are shown at the bottom. Mean performance was −12.8 dB for ES fibers displaying constant excitability, −8.1 dB for ES fibers displaying oscillating excitability, and +0.2 dB for AS fibers.

The effect of stimulus pulse rate on intensity discrimi-

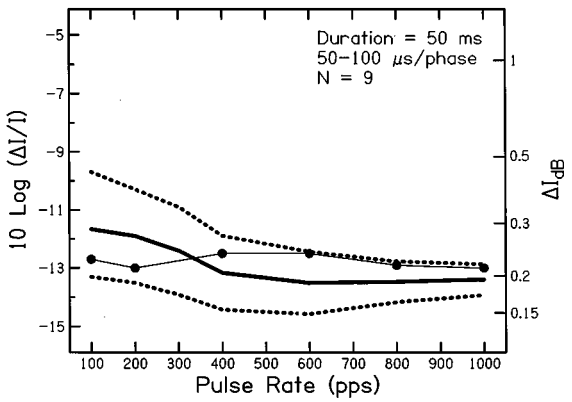

FIG. 12. Average intensity discrimination performance as a function of pulse rate for nine ES fibers from five animals, for 50 ms signals. Solid and dashed lines indicate mean ± 1 s.d. and filled symbols denote data from one of the fibers.

nation of 50 ms ES signals is shown in Fig. 12. Solid and dashed lines indicate mean ±1 s.d. for data from nine fibers in five animals, all of which were tested over the entire range of pulse rates. Filled symbols indicate data obtained from one of those fibers. Performance is not substantially different for pulse rates between 100 and 1000 pps. This might be expected on the basis of equivalent rate-level function slopes (when measured in absolute units of spikes/s/dB) and comparable spike count variability across pulse rate (Fig. 4).

III. DISCUSSION

A. ANF responses

Steeper rate-level functions and correspondingly reduced dynamic range in ES (Fig. 1) reflect the fact that direct electric stimulation is considerably more effective in eliciting spikes from spiral ganglion cells than synaptic neurotransmission. In addition, fibers can also respond at much higher sustained discharge rates in ES than in AS (Fig. 4). However, slopes of ES rate-level functions measured in absolute units of spikes/s/dB are generally no different at high pulse rates than at low pulse rates, and variability does not change. In terms of intensity discrimination, this implies that performance should not depend on pulse rate. This generalization holds for both single-fiber responses (Fig. 12) and psychophysical performance in implanted humans (Donaldson, personal communication).

Variability of both ES and AS spike counts conforms to Poisson-process predictions up to discharge rates of 20–40 spikes/s and then falls increasingly short of predicted behavior at higher discharge rates. Variability in AS conditions follows a monotonically increasing curve that resembles a power function. As noted earlier, several studies have shown that the discrepancy between observed behavior and Poisson-process predictions stems primarily from the effects of absolute and relative refractoriness. ES variability is smaller than AS variability in fibers whose excitability remains constant across time. Increasing pulse rate does not increase spike count variability in ES conditions, at least for pulse rates less than 800 pps in fibers capable of responding at high discharge rates (Fig. 4). Variability in ES responses is usually maximal at discharge rates of 100 spikes/s, and it often attains a plateau value that differs from fiber to fiber and is maintained throughout most of the remaining dynamic range. One of two behaviors occurs at high pulse and discharge rates, depending on the fiber's ability to respond in a sustained manner at discharge rates that exceed the stimulus pulse rate. For fibers that can do this, variability decreases to zero when responses become deterministic and each pulse elicits a spike. For fibers that cannot, variability increases when the discharge rate approaches the maximum possible rate. The maximum possible rate appears to depend on durations of absolute and relative refractory times, and these vary from fiber to fiber. ES variability becomes increasingly smaller than AS variability as discharge rates exceed 40 spikes/s, except in fibers exhibiting oscillating excitability.

Stochastic models of ES utilize rate-level functions whose shapes conform to integrated-Gaussian curves, and they predict a parabolic relationship between spike probability and variance in single-pulse and low-pulse-rate conditions (Bruce *et al.*, 1999). While some fibers exhibited parabolic variability functions for pulse rates of 200 pps (e.g., filled circles in Fig. 3), most did not. Also, parabolic variance curves were never observed in high-rate (>400 pps) stimulation, where refractory effects become significant. Bruce *et al.* (1999) showed that increasing absolute and relative refractory times flattens variability functions in predictable ways, and that choosing appropriate values can produce curves which conform to the observed data relatively well. An important point suggested by data presented here is that the duration of the absolute refractory period and the time constant of the relative refractory period both need to be increased substantially to account for ES variance curves. Furthermore, the existence of plateaus in many ES variability functions suggests that detailed shapes of rate-level functions differ for ES vs AS. That is, flattened variability functions argue that slopes of ES rate-level functions are constant over much of their extent. Our data also imply that integrated Gaussians, while convenient, do not describe shapes of ES rate-level functions precisely. That is, the facts that (1) ''true'' ES rate-level functions saturate at a very high discharge rates, (2) slopes do not vary appreciably across pulse rate, and (3) maximum possible discharge rates vary from fiber to fiber mean that low-pulse-rate stimuli only reveal part of the underlying function. Given this, a better description of ES rate-level functions would be provided by an integrated Gaussian that saturates at the maximum possible discharge rate, appropriately truncated at the stimulus pulse rate.

Related to the issue of internal noise, Rubinstein *et al.* (1997) presented preliminary neural modeling work that predicts a decrease in ES input–output slope when inter-spike intervals (ISIs) approach the absolute refractory time. The decreased slope stems from increased noise, which in turn arises because fewer ion channels are available for conducting spikes when ISIs are short. Thus as ISI decreases, neurons output spikes that have increasingly more variability, culminating in an inability to output any spikes when ISIs reach the absolute refractory time. The increase in variability we observed when neurons respond at their maximum possible rates (Fig. 4) is in general agreement with this concept. However, the observation that maximum possible discharge rates differ across fibers suggests corresponding differences in absolute and relative refractory times from cell to cell. Although our data suggest that these both increase in chronic profound deafness, a considerably larger sample size is needed to resolve this issue. The increased variability due to time-dependent fatigue (Fig. 8) apparently stems from a different source than refractoriness-related effects.

A recurrent theme in developing speech processing strategies for cochlear implants at the present time is that increasing pulse rates in each stimulation channel will change stochastic properties of ES responses such that they better approximate AS responses (Wilson *et al.*, 1994a). Changes in stochastic behavior can be approached from more than one point of view. On one hand, it can mean increased temporal spike dispersion, i.e., reduced phase-locking. However, since Hartmann and Klinke (1990) and Dynes and Delgutte (1992)

showed that ES responses to sinusoidal current are significantly phase-locked to at least 12 kHz, it appears that high-rate stimulation cannot substantially change this aspect of stochastic responsiveness. On the other hand, altered stochastic behavior can also mean increased spike count variability, as evidenced in PNDs with counts distributed over a larger range of values that better conform to Poisson-process predictions or AS behavior. Data in Fig. 4 show quite clearly that stimulation at rates up to 800 pps does not increase variability unless fibers discharge at their maximum possible rates, and even then the increase is relatively small. This suggests that increasing stimulation rates cannot alter the low-variability nature of intrinsic neural noise, and that a different approach is needed to increase variability. One way to achieve this is to add external noise to the signal (Wilson *et al.*, 1994b). While this certainly will succeed in increasing randomness, a problem is that all neurons activated by the signal will tend strongly to respond in a similar manner. However, although individual neurons may exhibit increased probabilistic response behavior when external noise is introduced, variability in the active neural population should not increase.

The phenomenon of ''oscillating excitability'' in ANF responses from chronically deafened ears (Figs. 6–7) has not been described previously. It resembles the ''rhythmic'' responses observed in auditory nerve activity in immature ears (e.g., Walsh and McGee, 1986). However, unlike responses of immature cells, oscillating excitability occurs at slower rates and its period varies with level. Although the proportion of fibers exhibiting oscillating excitability increased from 28% to 42% as duration of deafness increased from 6 to 12 weeks, our sample size is too small to draw firm conclusions about the prevalence of the phenomenon.

The origin of oscillating excitability is not clear. One possibility is that membrane potential slowly fluctuates over a wide range in de-afferented cells. Verveen's (1962) *in vitro* data, obtained intracellularly from frog sciatic nerve, show such fluctuations when voltage was clamped to high (-90 mV) potentials. This suggests the possibility that ion conductances responsible for resting potential change when de-afferentation silences a spiral ganglion cell. An interesting consequence of widely fluctuating membrane potentials is that cells may exhibit regular but low spontaneous discharge rates, even though the cell has no hair cell innervation. In our sample, several ANFs from deafened ears exhibited low (1–2 spikes/s) spontaneous activity that tended to occur at regular intervals.

It is also possible that oscillating excitability is a transient, ''start-up'' phenomenon which occurs only when electric signals force previously silent cells to respond, and it disappears when activity becomes frequent. Although oscillating excitability clearly occurs, more work is needed to establish its origin and impact on auditory perceptual processing in implanted humans.

B. Intensity discrimination

The difference in variability between ES and AS accounts for only about 4 dB of the large (approximately 13 dB) difference in intensity discrimination thresholds based on spike count.[2] The remainder reflects the steeper rate-level functions for ES. Rate-level functions for 200 pps signals in ES are 6–20 times steeper than those for CF tones in AS, as Fig. 1 illustrates. Consequently, a given intensity change produces a much larger change in count for ES, and the intensity change necessary to produce a criterion change in count is correspondingly smaller.

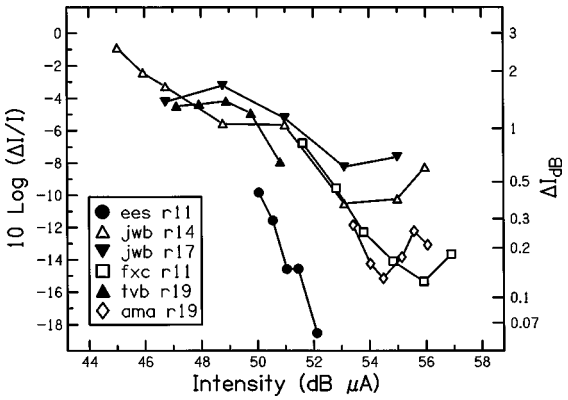

FIG. 13. Weber functions for intensity discrimination as a function of level by implanted humans, from Nelson *et al.* (1996). Different symbols denote data from different listeners. Corresponding values of ΔI_{dB} are shown on the (nonlinear) right axis for reference purposes.

Figure 13 shows human psychophysical data from Donaldson (personal communication) for ES intensity discrimination. Although the conditions are only partially comparable to those used in the present experiments,[3] it is interesting that the thresholds are similar to those shown for the ES neural data. Furthermore, by pooling selected fibers from Fig. 10 one can obtain a rough account of the psychophysical data, including the generally larger dynamic range. Such pooling would seem to require that responses of saturated fibers are ignored, similar to a situation that may exist in AS conditions (Viemeister, 1983, 1988; Delgutte, 1987; Winslow and Sachs, 1988).

The similarity between the ES neural data and the psychophysical data differs from the situation for AS. The Weber fraction for 50 ms, 1 kHz tones measured psychophysically is about -4 dB (Florentine, 1986)[4] versus -1 to $+2$ dB for data from individual cells (Fig. 10) and a mean performance of $+0.2$ dB across cells (Fig. 11). The smaller Weber fractions observed in psychophysical experiments can be reconciled with the neural data by assuming that spike counts are pooled over several fibers. More specifically, decisions based on optimally weighted counts from six to seven independent fibers would reduce the neural Weber fractions to those observed behaviorally. However, the major discrepancy between the neural and psychophysical AS data is not the difference in Weber fractions but the enormous difference in dynamic ranges. A multi-fiber, multi-population argument has been used to explain the psychophysical dynamic range for AS (Viemeister, 1988). Of course, the fiber populations involved in acoustic intensity coding would be different at different frequencies, and many fibers would be required to code intensity over the entire frequency and dynamic range of normal acoustic hearing.

The agreement between intensity discrimination perfor-

mance and dynamic range for ES fibers and implanted humans is surprising. Extending the argument above for AS, optimally weighting contributions from fewer than three ES fibers could reconcile the Weber fractions and the dynamic ranges. Although it is to be expected that deafness-induced cell loss would lead to fewer available fibers in implanted listeners, a functional population (per electrode) so small seems implausible. One possibility is that similar numbers of fibers are involved in ES and AS, but ES responses are not statistically independent. Rather, ES responses are positively correlated because of high synchronization to the pulsatile signals. In the limiting case, if responses across fibers were perfectly phase-locked and deterministic the Weber fraction for a combination of fibers would be the same as for one fiber.

Another possibility is that human performance is not determined by the stochastic behavior of ANF responses and that the major limitation is ''central noise,'' one source of which could be sub-optimal information weighting. In this case inputs from more than three fibers might be required to overcome the noise. This view suggests that the agreement between the human psychophysical data and physiological data from the auditory nerve is largely coincidental. Our opinion is that the agreement between neural and psychophysical performance in ES conditions is not coincidental. Rather, it is best explained by assuming statistical homogeneity in the population response to ES signals and in the dynamic ranges of active fibers.

Relative contributions of peripheral (stochastic) and central noise to perceptual performance could be examined by assessing intensity discrimination performance in ANF responses to stimulus conditions that affect randomness in peripheral activity. Two examples of these are long-pulsewidth signals (Dynes and Delgutte, 1992) and pulse rates >800 pps (Rubinstein *et al.*, 1997). With regard to the former, Ferguson *et al.* (1998) found that variability in behavioral thresholds to electrical stimuli increases with pulsewidth, in accord with ANF data and stochastic neural models. This suggests that peripheral neural processing plays a larger role than central processing, at least for tasks related to absolute threshold, and that central noise is both constant and of smaller magnitude than peripheral/stochastic noise. However, sufficient data to address the roles of peripheral versus central noise in other tasks, one of which is intensity discrimination, are not yet available.

ACKNOWLEDGMENTS

This work was supported in part by Grants Nos. P01 DC00110 and R01 DC00138 from NIDCD. The authors gratefully acknowledge the assistance of Robert K. Shepherd and Dan Clark in collecting the neural data, Gangesh K. Ganesan in conducting preliminary analyses (Ganesan, 1996), Gail S. Donaldson and David A. Nelson in providing the human psychophysical data, and two anonymous reviewers for their comments. Portions of this work were presented at the 21st Mid-Winter Meeting of the Association for Research in Otolaryngology (Viemeister *et al.*, 1998).

[1]Weber functions for ES must be U-shaped, similar to those shown for AS. They do not appear this way in the upper panel of Fig. 10 because for intensities eliciting discharge rates at and near the stimulus pulse rate, no value of ΔI produced the increase in discharge rate needed to estimate a difference limen. Hence, Weber fractions could not be estimated. This situation is particularly prevalent in ES because, unlike the situation in AS, discharge rate saturates abruptly at the pulse rate for low-rate (<600 pps) signals.

[2]To see this, consider performance in terms of d' rather than $P(C)$. For the present situation in which decisions are based on spike count,

$$d' = \frac{c(I+\Delta I) - c(I)}{\sigma_c},$$

where $c(I+\Delta I)$ and $c(I)$ are mean counts elicited by two signals differing in intensity and σ_c is the standard deviation of the counts at intensity I, assuming equal variance and a constant counting interval. Assuming linearity of the rate-level function in the coordinates of Fig. 1, this becomes

$$d' = \frac{S\Delta I_{\mathrm{dB}} T}{\sigma_c},$$

where S is the slope of the rate-level function in spikes/s/dB and T is the counting interval. From Fig. 2, σ_c is lower by approximately a factor of 2 for ES than for AS when I is within the dynamic range of the fiber. This reduction in variability increases d' by a factor of 2. For 50 ms signals, rate-level functions in ES are approximately 10 times steeper than those in AS when measured in absolute units of spikes/s/dB and estimated at the steepest portion of the function. Thus for a given change in level the overall d' should be a factor of 20 greater for ES. To express this in terms of discrimination thresholds, note that d' is proportional to ΔI_{dB} so, for the same d', ΔI_{dB} will be reduced by a factor of 2 by the reduction in σ_c and by 10 by the increase in S. From Fig. 5, ΔI_{dB} is approximately 3.2 dB for AS. The factor of 2 reduction decreases the Weber fraction by 3.9 dB (to -3.5 dB), and the factor of 10 reduction further decreases the Weber fraction by 10.5 dB (to -14.0 dB).

[3]The stimuli used by Nelson *et al.* (1996) were 200 μs phase, 125 pps biphasic pulse trains presented for 300 ms, and a 3IFC tracking procedure was employed to estimate the DL that yielded $P(C)=0.794$ ($d'=1.63$). The data shown in Fig. 13 were obtained with 100 μs phase, 200 pps biphasic pulse trains presented for 50 ms, and the DL was estimated for $P(C)=0.70$ in 2IFC ($d'=0.75$). Decreasing pulse duration from 200 to 100 μs phase would not affect the psychophysical DLs at equal sensation levels, nor would changing the pulse rate from 125 to 200 Hz (Donaldson, personal communication). Based on acoustic data (Florentine, 1986), decreasing duration from 300 ms to 50 ms would increase the Weber fraction by approximately 2 dB. The psychometric functions presented in Nelson *et al.* (1996) indicate that d' is a linear function of ΔI. Thus the Weber fraction would be reduced by $10\log(1.63/0.75)=3.4$ dB for $P(C)=0.7$ in 2IFC. The net result is that if the psychophysical data had been obtained under conditions comparable to those used for the neural data, the Weber fractions would be reduced by $3.4-2=1.4$ dB.

[4]Florentine (1986) used a 2IFC adaptive procedure that estimated the DL for $P(C)=0.71$. This performance level is nearly identical to the 0.70 value used to define DLs in our analysis. It is well known that acoustic Weber fractions decrease with the intensity of the standard, and it appears that this ''near miss'' to Weber's Law results from the nonlinear spread of excitation to frequency regions remote from that of the standard (for a review, see Plack and Carlyon, 1995). Florentine obtained a Weber fraction of -4 dB at 1 kHz and 40 dB SPL, the lowest level used in that study. We use the Weber fraction at this level because it is least likely to be affected by nonlinear spread of excitation and thus is comparable to the situation that likely exists throughout the lower part of the dynamic range in ES.

Bruce, I. C., Irlicht, L. S., White, M. W., O'Leary, S. J., Dynes, S., Javel, E., and Clark, G. M. (**1997**). ''A stochastic model of the electrically stimulated auditory nerve designed for the analysis of large-scale population response,'' Abst. Assn. Res. Otolaryngol. **20**, 57.

Bruce, I. C., Irlicht, L. S., White, M. W., O'Leary, S. J., Dynes, S., Javel, E., and Clark, G. M. (**1999**). ''A stochastic model of the electrically stimulated auditory nerve: Pulse-train response,'' Proc. IEEE Trans. Biomed. Eng. **46**, 630–637.

Delgutte, B. (**1987**). ''Peripheral auditory processing of speech information: Implications from a physiological study of intensity discrimination,'' in *The Psychophysics of Speech Perception*, edited by M. E. H. Schouten (Nijhoff, Dordrecht, The Netherlands), pp. 333–353.

Donaldson, G. S. (**1998**). Personal communication.
Donaldson, G. D., Viemeister, N. F., and Nelson, D. A. (**1997**). ''Psychometric functions and temporal integration in electric hearing,'' J. Acoust. Soc. Am. **101**, 3706–3721.
Dynes, S. B. C., and Delgutte, B. (**1992**). ''Phase-locking of auditory-nerve discharges to sinusoidal electric stimulation of the cochlea,'' Hearing Res. **58**, 79–90.
Ferguson, W. D., Smith, D. W., Finley, C. C., Pfingst, B. E., and Collins, L. M. (**1998**). ''Prediction of the variance in behavioral thresholds using a stochastic model of electrical stimulation,'' Abst. Assn. Res. Otolaryngol **21**, 290.
Florentine, M. (**1986**). ''Level discrimination of tones as a function of duration,'' J. Acoust. Soc. Am. **79**, 792–798.
Ganesan, G. K. (**1996**). ''Analyses and comparison of the responses of single ANFs to acoustic and electric stimulation,'' M.S. Thesis, University of Minnesota.
Gaumond, R. P., Molnar, C. E., and Kim, D. O. (**1982**). ''Stimulus and recovery dependence of cat cochlear nerve fiber spike discharge probability,'' J. Neurophysiol. **48**, 856–873.
Gray, P. R. (**1967**). ''Conditional probability analyses of the spike activity of single neurons,'' Biophys. J. **7**, 759–777.
Hartmann, R., and Klinke, R. (**1990**). ''Response characteristics of nerve fibers to patterned electrical stimulation,'' in *Models of the Electrically Stimulated Cochlea*, edited by J. M. Miller and F. A. Spelman (Springer-Verlag, New York), pp. 135–159.
Hartmann, R., Topp, G., and Klinke, R. (**1984**). ''Electrical stimulation of the cat cochlea: Discharge pattern of single auditory fibers,'' Adv. Audiol. **1**, 18–29.
Javel, E. (**1990**). ''Acoustic and electrical encoding of temporal information,'' in *Models of the Electrically Stimulated Cochlea*, edited by J. M. Miller and F. A. Spelman (Springer-Verlag, New York), pp. 247–292.
Javel, E., and Shepherd, R. K. (**1999**). ''Electrical stimulation of the auditory nerve. III. Response initiation sites and temporal fine structure,'' Hearing Res. (in press).
Javel, E., Tong, Y. C., Shepherd, R. K., and Clark, G. M. (**1987**). ''Responses of cat ANFs to biphasic electrical current pulses,'' Ann. Otol. Rhinol. Laryngol. **96** Suppl. 128, 26–30.
Johnson, D. H., and Swami, A. (**1983**). ''The transmission of signals by auditory-nerve fiber discharge patterns,'' J. Acoust. Soc. Am. **74**, 493–501.
Leake, P. A., and Hradek, G. T. (**1988**). ''Cochlear pathology of long term neomycin induced deafness in cats,'' Hearing Res. **33**, 11–34.
Liberman, M. C. (**1982**). ''The cochlear frequency map for the cat: Labeling ANFs of known characteristic frequency,'' J. Acoust. Soc. Am. **75**, 1441–1449.
Liberman, M. C. (**1980**). ''Morphological differences among radial afferent fibers in the cat cochlea: An electron-microscopic study of serial sections,'' Hearing Res. **3**, 45–63.
Liberman, M. C., and Oliver, M. E. (**1984**). ''Morphometry of intracellularly labeled neurons of the auditory nerve: Correlations with functional properties,'' J. Comp. Neurol. **223**, 163–176.
Movshon, J. A., Tolhurst, D. J., and Dean, A. F. (**1982**). ''How many neurons are involved in perceptual decisions?'' Invest. Ophthalmol. Visual Sci. **22**, 207.
Moxon, E. C. (**1971**). ''Neural and mechanical responses to electric stimulation of the cat's inner ear,'' Doctoral thesis, MIT.
Nelson, D. A., Schmitz, J. L., Donaldson, G. S., Viemeister, N. F., and Javel, E. (**1996**). ''Intensity discrimination as a function of stimulus level with electric stimulation,'' J. Acoust. Soc. Am. **100**, 2393–2414.
Plack, C. J., and Carlyon, R. P. (**1995**). ''Loudness perception and intensity coding,'' in *Hearing*, edited by B. C. J. Moore (Academic, New York), pp. 1223–160.
Relkin, E. M., and Pelli, D. G. (**1987**). ''Probe tone thresholds in the auditory nerve measured by two-interval forced-choice procedures,'' J. Acoust. Soc. Am. **82**, 1679–1691.
Rubinstein, J. T., Matsuoka, A. J., Abbas, P. J., and Miller, C. A. (**1997**). ''The neurophysiological effects of simulated auditory prosthesis stimulation,'' Second quarterly progress report (NIH Contract N01 DC-6-2111).
Sachs, M. B., and Abbas, P. J. (**1974**). ''Rate versus level functions for auditory-nerve fibers in cats: Tone-burst stimuli,'' J. Acoust. Soc. Am. **56**, 1835–1847.
Sachs, M. B., Winslow, R. L., and Sokolowski, B. H. A. (**1989**). ''A computational model for rate-level functions from cat auditory-nerve fibers,'' Hearing Res. **41**, 61–69.
Shannon, R. V. (**1993**). ''Psychophysics,'' in *Cochlear Implants: Audiological Foundations*, edited by R. S. Tyler (Singular, San Diego, CA), pp. 357–388.
Shepherd, R. K., and Javel, E. (**1997**). ''Electrical stimulation of the auditory nerve. I. Correlation of physiological responses with cochlear status,'' Hearing Res. **108**, 112–144.
Spoendlin, H., and Schrott, A. (**1989**). ''Analysis of the human auditory nerve,'' Hearing Res. **43**, 25–38.
Teich, M. C., and Khanna, S. M. (**1985**). ''Pulse number distribution for the neural spike train in the cat's auditory nerve,'' J. Acoust. Soc. Am. **77**, 1110–1128.
Verveen, A. A. (**1962**). ''Axon diameter and fluctuation in excitability,'' Acta Morphol. Neerlando-Scand. **5**, 79–85.
Viemeister, N. F. (**1983**). ''Auditory intensity discrimination at high frequencies in the presence of noise,'' Science **221**, 1206–1208.
Viemeister, N. F. (**1988**). ''Psychophysical aspects of auditory intensity coding,'' in *Auditory Function: Neurobiological Bases of Hearing*, edited by G. M. Edelman, W. E. Gall, and W. M. Cowan (Wiley, New York), pp. 213–242.
Viemeister, N. F., Javel, E., and Ganesan, G. K. (**1998**). ''Auditory nerve correlates of intensity discrimination for electrical stimuli,'' Abst. Assn. Res. Otolaryngol. **21**, 289.
Walsh, E. J., and McGee, J. (**1986**). ''The development of function in the auditory periphery,'' in *Neurobiology of Hearing: The Cochlea*, edited by R. A. Altschuler, R. P. Bobbin, and D. W. Hoffman (Raven, New York), pp. 247–282.
Westerman, L. A., and Smith, R. L. (**1984**). ''Rapid and short term adaptation in auditory-nerve responses,'' Hearing Res. **15**, 249–260.
White, M. W., Finley, C. C., and Wilson, B. S. (**1987**). ''Electrical stimulation of the auditory nerve: Stochastic response characteristics,'' in I.E.E.E. 9th Annual Conference of the Engineering in Medicine and Biology Society, pp. 1906–1907.
Wilson, B. S., Finley, C. C., Zerbi, M., and Lawson, D. T. (**1994a**). ''Speech processors for auditory prostheses,'' Seventh quarterly progress report (NIH Contract N01 DC-2-2401).
Wilson, B. S., Finley, C. C., Zerbi, M., and Lawson, D. T. (**1994b**). ''Speech processors for cochlear prostheses,'' Ninth quarterly progress report (NIH Contract N01 DC-2-2401).
Winslow, R. L., and Sachs, M. B. (**1988**). ''Single-tone intensity discrimination based on auditory-nerve rate responses in backgrounds of quiet, noise, and with stimulation of the crossed olivocochlear bundle,'' Hearing Res. **35**, 165–189.
Winter, I. M., and Palmer, A. R. (**1991**). ''Intensity coding in low-frequency auditory-nerve fibers of the guinea pig,'' J. Acoust. Soc. Am. **90**, 1958–1967.
Xu, S. A., Shepherd, R. K., Chen, Y., and Clark, G. M. (**1993**). ''Deaf animal models: Profound hearing loss in the cat following a single coadministration of kanamycin and ethacrynic acid,'' Hearing Res. **70**, 205–215.
Young, E. D., and Barta, P. E. (**1986**). ''Rate responses of ANFs to tones in noise near masked threshold,'' J. Acoust. Soc. Am. **79**, 426–442.